Journal of Sound and Vibration (1997) **199**(2), 275–284

VIBRATION ANALYSIS OF LAMINATED BEAMS USING AN ITERATIVE SMEARED LAMINATE MODEL

J. A. Zapfe

Kinetic Systems, Inc., 20 *Arboretum Road, Boston, MA* 02131, *U.S.A.*

AND

G. A. Lesieutre

Department of Aerospace Engineering, The Pennsylvania State University, University Park, PA 16802, U.S.A.

(*Received* 28 *December* 1995, *and in final form* 20 *May* 1996)

A smeared laminate model is presented for the dynamic analysis of laminated beams. An iterative process is used to refine successively the shape of the assumed displacement field in the beam, resulting in a self-consistent stress/strain distribution. The model includes the effects of transverse shear and rotatory inertia. The iterative model is used to predict the modal frequencies and damping of simply supported beams with integral viscoelastic layers. The solutions for a three layer beam are compared to a three layer approximate model. A nine layer solution is also presented, illustrating the applicability of the model to multi-layer configurations, situations that would normally require a more complex, discrete layer analysis.

1. INTRODUCTION

Accurate modeling of the stress distribution in general composite beams, plates and shells typically requires the inclusion of such non-classical effects as transverse shear deformation and transverse normal strain. Accurate estimates of the stress field are particularly important in damping and delamination studies. Displacement models which go beyond the assumptions of Classical Lamination Theory (CLT) are generally classified as either Smeared Laminate Models (SLMs) or Discrete Layer Models (DLMs).

In a SLM, a form of the displacement field is assumed through the entire thickness of the laminate. This specification of the displacement field allows the calculation of a set of equivalent laminate properties (such as the [A], [B] and [D] matrices in CLT) which can be used to determine the gross behavior of the laminate (such as the deflection and natural frequency). Examples of SLM's are: First Order Shear Deformation Theory (FSDT) as presented by Yang, Norris and Stavsky [1]; quadratic shear strain models as presented by Krishna Murty [2], Levinson [3, 4] and Reddy [5]; and the more recent "zig-zag" models as presented by Di Sciuva [6] and Bhaskar and Varadan [7]. The limitation of smeared laminate models, when applied to general laminate configurations, is the implicit assumption of the shape of the stress distribution which follows from the assumption of the displacement field. If the assumed stress distribution is not representative of the actual stress field, then the predictions of a smeared laminate model can be significantly in error. Accurate determination of the stress and displacement fields is particularly important for "stress critical" calculations such as damping and delamination.

0022–460X/97/020275 + 10 $25.00/0/sv960631

In a DLM, a form of the displacement field is assumed at the ply level only. DLMs retain the individuality of the ply throughout the analysis and are readily adaptable to general laminate configurations. DLMs are also distinguished by their requirement for large numbers of degrees of freedom, usually proportional to the number of plies in the laminate. DLMs were presented by Ross *et al*. [8], Sun and Whitney [9], Alam and Asnani [10] and Reddy [11].

SLMs are generally preferable to DLMs because they use fewer degrees of freedom. However, because SLMs contain an implicit assumption of the shape of the stress distribution, often there is no choice but to use a more numerically intensive DLM for accurate stress predictions.

Although the stress field obtained using a SLM is related to the assumed displacement field, the local stress solution can be refined somewhat by using the equations of elemental stress equilibrium. Noor and Burton [12] presented a "predictor-corrector" approach for the analysis of composite plates. The authors used a plate model based on FSDT, coupled with integration of the equilibrium equations, to refine the estimate of the local stress field through the thickness of the laminate. The refined stress field was also used to generate improved estimates of the shear correction factors in the FSDT model, leading to improved estimates of the plate displacements and natural frequencies. While the approach presented by Noor and Burton does lead to improved estimates of the stress distribution, the accuracy of the local stress solution is ultimately limited by the initial FSDT displacement assumption.

Vijayakumar and Krishna Murty [13] developed a SLM for the static analysis of laminated plates that could, in fact, accurately predict the stress distribution in general laminates. The authors used an iterative process to successively refine the stress/strain field in the laminate. Vijayakumar and Krishna Murty's results for composite cross-ply plates exhibited excellent agreement with exact solutions.

Zapfe and Lesieutre [14] presented a variation of Vijayakumar and Krishna Murty's static method for laminated beams. Zapfe and Lesieutre used an assumed displacement approach which produced differential equations of equilibrium and boundary conditions similar to other SLMs, and used iteration to successively improve the estimate of the assumed displacement field.

The present research extends the iterative SLM (ISLM) developed by Zapfe and Lesieutre to the dynamic analysis of laminated beams. The current model is developed for the specific case of simply supported beams with uniform properties along the length. The model is used to analyze the dynamics of two sample beams with integral viscoelastic layers.

2. THEORY

Figure 1 depicts the beam configuration for the ISLM. The material properties may vary in the thickness direction, but are assumed to be constant along the length of the beam.

The form of the displacement field over the domain of the beam is

$$u(x, z, t) = u_0(x, t) - z\,\partial w(x, t)/\partial x + f(z)g(x, t), \qquad w(x, z, t) = w(x, t). \tag{1}$$

The first two terms in the in-plane displacement expression define the CLT displacement field for a beam. The last term, $f(z)g(x, t)$, can be thought of as a correction to account for transverse shear effects. The function $f(z)$ represents the shape of the correction through the thickness of the beam, while $g(x, t)$ determines its distribution along the length. The transverse displacement field, $w(x, t)$, is not a function of z, which means the transverse

normal strain is identically zero. The solution of a given problem requires the determination of the unknown functions, $u_0(x, t)$, $w(x, t)$, $g(x, t)$ and $f(z)$.

In the present model, $f(z)$ does not generally have a simple form. However, some familiar smeared laminated models can be expressed by the displacement field given in equation (1):

$$\text{CLT: } f(z) = 0, \qquad \text{FSDT: } f(z) = z,$$
$$\text{Levinson/Reddy: } f(z) = -6h_l h_u z + 3(h_l + h_u)z^2 - 2z^3. \tag{2}$$

The strain field in the beam provides some insight into the nature of the function $f(z)$. Applying the linear strain/displacement relations to equation (1) yields the strain field

$$\varepsilon_x(x, z, t) = \partial u/\partial x = \partial u_0/\partial x - z\,\partial^2 w/\partial x^2 + f(z)\,\partial g/\partial x,$$
$$\varepsilon_z(x, z, t) = \partial w/\partial z = 0, \qquad \gamma_{xz}(x, z, t) = \partial u/\partial z + \partial w/\partial x = \partial f/\partial z\; g(x, t). \tag{3}$$

From equation (3), it can be seen that the gradient $\partial f/\partial z$ represents the shape of the transverse shear strain field through the thickness of the laminate, at a given x-location. Therefore, if the shape of the shear strain distribution is known, $f(z)$ can be estimated by integrating the strain through the thickness. In general there will be no closed form solution for $f(z)$. In the present analysis, $f(z)$ is stored as a tabular function, with an assigned numerical value at a set of pre-defined z-locations.

2.1. DIFFERENTIAL EQUATIONS OF MOTION AND BOUNDARY CONDITIONS

While the assumed form of the shear correction, $f(z)$, will change from one iteration to the next, at any given iteration it can be treated as a known function. This allows the development of differential equations and boundary conditions like any other SLM. The strain energy stored in the beam has components associated with both extension and shear and is given by

$$U = \frac{b}{2}\int_0^L \int_{h_l}^{h_u} E(z)\varepsilon_x^2(x, z, t) + G(z)\gamma_{xz}^2(x, z, t)\,\mathrm{d}x\,\mathrm{d}z. \tag{4}$$

The kinetic energy, which includes components associated with transverse, in-plane and rotary inertia, is given by

$$T = \frac{b}{2}\int_0^L \int_{h_l}^{h_u} \rho(z)\left[\left(\frac{\partial u(x, z, t)}{\partial t}\right)^2 + \left(\frac{\partial w(x, t)}{\partial t}\right)^2\right]\mathrm{d}x\,\mathrm{d}z, \tag{5}$$

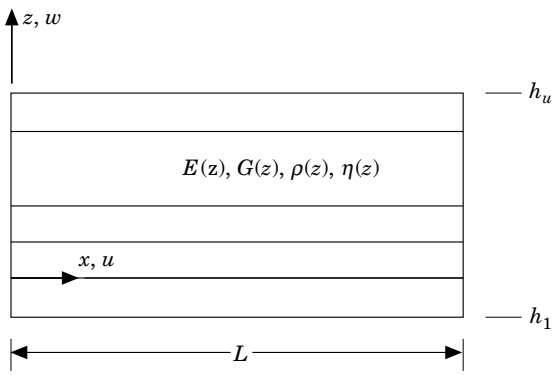

Figure 1. Beam configuration for the Iterative Smeared Laminate Model; b = width.

where the in-plane velocity, $\partial u/\partial t$, is given by

$$\partial u(x, z, t)/\partial t = \partial u_0(x, t)/\partial t - z\,\partial^2 w(x, t)/\partial x\,\partial t + f(z)\,\partial g(x, t)/\partial t. \tag{6}$$

The differential equations of motion and boundary conditions are derived using Hamilton's principle. The equations of motion for the three unknown functions u_0, w and g are

$$\begin{aligned} -M_1\ddot{u}_0 + M_2\ddot{w}' - M_3\ddot{g} &= -K_1u_0'' + K_2w''' - K_3g'', \\ -M_2\ddot{u}_0' + M_4\ddot{w}'' - M_1\ddot{w} - M_5\ddot{g}' &= -K_2u_0''' + K_4w^{iv} - K_5g''', \\ -M_3\ddot{u}_0 + M_5\ddot{w}' - M_6\ddot{g} &= -K_3u_0'' + K_5w''' - K_6g'' + \mathrm{K}_7\mathrm{g}. \end{aligned} \tag{7}$$

$K_{1\text{–}7}$ and $M_{1\text{–}6}$ are section stiffness and mass coefficients, given by

$$K_{[1,2,3,4,5,6]} = b\int_{h_l}^{h_u} E(z)[1, z, f(z), z^2, zf(z), f^2(z)]\,\mathrm{d}z, \qquad K_7 = b\int_{h_l}^{h_u} G(z)\left[\frac{\partial f(z)}{\partial z}\right]^2\mathrm{d}z,$$

$$M_{[1,2,3,4,5,6]} = b\int_{h_l}^{h_u} \rho(z)[1, z, f(z), z^2, zf(z), f^2(z)]\,\mathrm{d}z. \tag{8}$$

In general, the section integrals will not have closed form solutions. In the present implementation, the integrals are evaluated numerically using a trapezoidal method.

The kinematic and natural boundary conditions, specified at $x = 0$ and $x = L$, are given by

KINEMATIC		NATURAL
Specify: u_0	or	$K_1u_0' - K_2w'' + K_3g' = 0,$
Specify: w	or	$M_2\ddot{u}_0 - M_4\ddot{w}' + M_5\ddot{g} - K_2u_0'' + K_4w''' - K_5g'' = 0,$
Specify: w'	or	$-K_2u_0' + K_4w'' - K_5g' = 0,$
Specify: g	or	$K_3u_0' - K_5w'' + K_6g' = 0.$

(9)

For the special case of a simply supported beam, the first, third and fourth natural boundary conditions are combined with the kinematic boundary condition, $w = 0$.

2.2. SOLUTION FOR A SIMPLY SUPPORTED BEAM

The special case of a simply supported beam leads to simple harmonic solution functions. Functions which satisfy the boundary conditions and the differential equations of motion are:

$$u_0(x, t) = U_0\,\mathrm{e}^{(\mathrm{i}\omega_n t)}\cos(k_n x), \qquad w(x, t) = W_0\,\mathrm{e}^{(\mathrm{i}\omega_n t)}\sin(k_n x),$$
$$g(x, t) = G_0\,\mathrm{e}^{(\mathrm{i}\omega_n t)}\cos(k_n x). \tag{10}$$

The functions are solutions provided the wave number, $k_n = n\pi/L$ corresponds to an integer number of 1/2 waves along the length of the beam. The values of the complex frequency and the unknown coefficients U_0, W_0 and G_0 are found by substitution of equations (10) into the differential equations of motion, equations (7). The substitution leads to the following eigenvalue problem:

$$[-\omega_n^2[M] + [K]]\{U\} = \{0\}, \qquad \{U\} = \{U_0, W_0, G_0\}^{\mathrm{T}}$$

$$[M] = \begin{bmatrix} M_1 & -M_2 k_n & M_3 \\ -M_2 k_n & (M_1 + M_4 k_n^2) & -M_5 k_n \\ M_3 & -M_5 k_n & M_6 \end{bmatrix}, \quad [K] = \begin{bmatrix} K_1 k_n^2 & -K_2 k_n^3 & K_3 k_n^2 \\ -K_2 k_n^3 & K_4 k_n^4 & -K_5 k_n^3 \\ K_3 k_n^2 & -K_5 k_n^3 & (K_6 k_n^2 + K_7) \end{bmatrix}. \tag{11}$$

The eigensolution yields three frequencies and mode shapes for each wave number. The eigenvalue with the lowest frequency typically corresponds to the transverse mode.

2.3. DISSIPATION MODEL

The complex modulus method is used to model energy dissipation. The Young's and shear modulus of the constituent materials are represented by the complex quantities

$$E^*(z) = E(z)[1 + \mathrm{i}\eta(z)], \qquad G^*(z) = G(z)[1 + \mathrm{i}\eta(z)]. \tag{12}$$

The ISLM can readily accomodate different loss factors for shear and dilation.

The complex modulus formulation leads to complex section stiffness coefficients in equation (8) and complex eigenvalues and eigenvectors in equation (11). The complex eigenvalue yields both frequency and damping information. The complex eigenvector contains magnitude and phase information for the mode shape. The modal loss factor for the nth mode is given by

$$\eta_n = \mathrm{Im}(\omega_n^2)/\mathrm{Re}(\omega_n^2). \tag{13}$$

2.4. IMPROVED ESTIMATE FOR SHEAR CORRECTION FUNCTION $f(z)$

An improved estimate for the shear correction function, $f(z)$, is derived from the transverse shear stress distribution as determined from the equation of elemental stress equilibrium. Stress equilibrium imposes a relationship between the transverse shear stress gradient, the in-plane normal stress gradient and the in-plane inertial stress gradient:

$$\partial\tau_{xz}/\partial z = \rho\ddot{u} - \partial\sigma_x/\partial x. \tag{14}$$

The terms on the right hand side of equation (14) are known from the eigensolution to equation (11). The inertial stress gradient is given by

$$\rho\ddot{u} = -\rho(z)\omega_n^2[U_0 - k_n z W_0 + f(z)G_0]\,\mathrm{e}^{(\mathrm{i}\omega_n t)}\cos(k_n x), \tag{15}$$

and the in-plane normal stress gradient is given by

$$\partial\sigma_x/\partial x = -E(z)k_n^2[U_0 - k_n z W_0 + f(z)G_0]\,\mathrm{e}^{(\mathrm{i}\omega_n t)}\cos(k_n x). \tag{16}$$

The transverse shear stress gradient is obtained by substitution of equations (15) and (16) into equation (14):

$$\partial\tau_{xz}/\partial z = [-\rho(z)\omega_n^2 + E(z)k_n^2][U_0 - k_n z W_0 + f(z)G_0]\,\mathrm{e}^{(\mathrm{i}\omega_n t)}\cos(k_n x). \tag{17}$$

The shear stress gradient is a separable function of x, z and t. The shape of the shear stress gradient through the thickness is the same at every x-location along the beam, with magnitude varying spatially by $\cos(k_n x)$ and harmonically in time. The shape of the shear stress distribution can be found by integrating equation (17) through the thickness.

$$\tau_{xz}(z) = \int_{h_l}^{z} [-\rho(z)\omega_n^2 + E(z)k_n^2][U_0 - k_n z W_0 + f(z)G_0]\,\mathrm{d}z. \tag{18}$$

The shear stress is influenced by both elastic and inertial effects, the relative importance of each depending on the mode. The elastic component typically predominates, except at

very high frequency. In general, the shear stress distribution has no closed form solution. In the present implementation, the integration is performed numerically using a trapezoidal method.

The shape of the shear strain distribution is calculated using equation (18) and the constitutive relation

$$\gamma_{xz}(z) = \tau_{xz}(z)/G(z). \tag{19}$$

The shear strain can be a complex quantity, with the implication that all parts of the beam do not necessarily move in phase with each other.

The new estimate for the shear correction function, $f(z)$, obtained by integrating equation (19) through the thickness, is given by

$$f(z) = \int_{h_l}^{z} \gamma_{xz}(z)\,\mathrm{d}z + F_0, \tag{20}$$

where the constant, F_0, is required to ensure that $f(z) = 0$ at the reference axis. The integral in equation (20) is evaluated numerically and $f(z)$ can be a complex quantity. This new estimate of $f(z)$ is used as the shear correction function for the next iteration. The solution steps for subsequent iterations are identical.

2.5. CONVERGENCE TO A SOLUTION

As with any smeared laminate model, there are two distinct ways to calculate the shear stress distribution: from the material constitutive relations; or by elemental stress equilibrium. For the simply supported beam, these two shear distributions are given by

$$\text{Constitutive: } \tau_{xz} = G(z)\partial f(z)/\partial z G_0,$$

$$\text{Equilibrium: } \tau_{xz} = \int_{h_l}^{z} [-\rho(z)\omega_n^2 + E(z)k_n^2][U_0 - k_n z W_0 + f(z)G_0]\,\mathrm{d}z. \tag{21}$$

The ultimate goal of the iterative analysis is the determination of the function, $f(z)$, that causes the two stress distributions to be equal. This defines the convergence point for the iterative function $f(z)$, the point at which the stresses and strains are self-consistent. In the present development, the transverse shear resultants, given by

$$V_{\text{Constitutive}} = \int_{h_l}^{h_u} [\tau_{xz}]_{\text{Constitutive}}\,\mathrm{d}z, \qquad V_{\text{Equilibrium}} = \int_{h_l}^{h_u} [\tau_{xz}]_{\text{Equilibrium}}\,\mathrm{d}z, \tag{22}$$

are used as the measure of convergence. When the magnitude of the error between the two resultants reaches a given tolerance (typically 1% of the equilibrium resultant) then the solution is considered to have converged. Although the shear resultant is an integral quantity which does not necessarily reflect local errors in the stress field, the authors have found it to be a reliable measure. While other error measures can be devised, the shear resultant has a physical significance which is particularly useful in static problems.

2.6. CHOICE OF $f(z)$ FOR FIRST ITERATION

Since $f(z)$ is determined from the previous iteration, the question arises as to what to use for the first iteration. Almost any reasonable displacement assumption is acceptable. FSDT [$f(z) = z$] is simple to implement, however experience has shown that a quadratic stress distribution is a better starting point. This is likely due to the fact that the parabolic

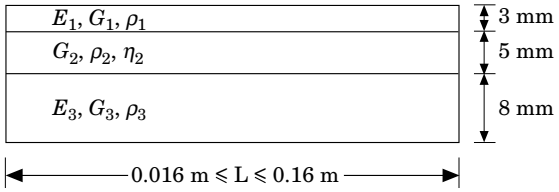

Figure 2. Beam configuration for three layer example. The material properties are $E_1 = E_3 = 2{\cdot}068E11$ Pa, $G_1 = G_3 = 8{\cdot}272$ E10 Pa, $\rho_1 = \rho_3 = 7850$ kg/m^3; $G_2 = 9{\cdot}8$ E9 Pa, $\rho_2 = 2600$ kg/m^3, $\eta_2 = 0{\cdot}1$. The beam is simply supported at both ends.

stress field produces a continuous shear stress distribution which places shear stress in all of the layers. With the FSDT starting point, the shear stress is very small in layers having a low shear modulus.

3. RESULTS AND DISCUSSION

Rao [15] assembled a series of design curves for the dynamic characterization of three layer sandwich beams with various boundary conditions. Rao uses the differential equations of motion for a sandwich beam that were presented by Mead and Markus [16]. The beam model assumes that all transverse shear deformation and energy dissipation occurs in the core material. The dissipation is modeled using a complex modulus formulation. The imposition of boundary conditions leads to a sixth order characteristic determinant which Rao solves numerically. The ISLM was compared to Rao's design curves for the first examples presented in Rao's paper, with simply supported boundary conditions. To illustrate its capabilities, the ISLM was also used to analyze a nine layer version of Rao's beam.

3.1. THREE LAYER EXAMPLE

The beam configuration for Rao's first example appears in Figure 2. The beam geometry and material properties are summarized in the figure. The length of the beam was varied by a factor of ten in order to obtain a range of frequencies for the first transverse mode.

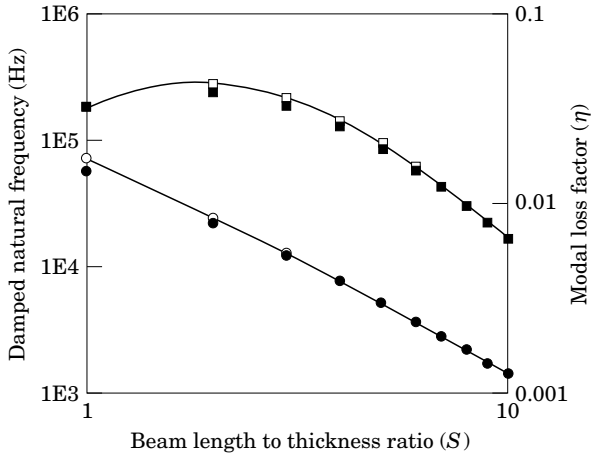

Figure 3. Modal data for mode 1 of three layer example using ISLM and Rao's design curves: ○, Rao frequency; □, Rao loss factor; ●, ISLM frequency; ■, ISLM loss factor.

TABLE 1

Iterative improvement of modal data for a three layer beam

	Quadratic shear		FSDT	
Iteration Number	Frequency Error (%)	Loss Factor Error (%)	Frequency Error (%)	Loss Factor Error (%)
1	0·22	−1·42	9·6	−97·9
2	0·0	0·0	0·01	−0·22
3	0·0	0·0	0·0	−0·0002

Figure 3 shows the predicted modal frequency and loss factor for the three layer beam using Rao's design curves and the ISLM. The ISLM frequency predictions are generally consistent with Rao's results. The slight discrepancy at high frequency is due to facesheet shear and rotary inertia, effects which Rao's model does not consider. With rotatory inertia and facesheet shear removed, the ISLM replicates Rao's results. The modal loss factors predicted by the ISLM are also in good agreement with Rao's results. Again the slight discrepancy is due to facesheet shear and rotary inertia.

Table 1 shows the improvement in the prediction of the modal data for the three layer example using two different starting points for the first iteration: a quadratic shear stress; and a constant shear strain (FSDT displacement field). The data corresponds to a beam length-to-thickness ratio, $S = 5$. In this particular example, for the first iteration, the quadratic shear stress assumption is adequate in itself: the frequency prediction is within 0·22% of the converged value and the loss factor is within 1·42%. The second iteration corrects both errors. The FSDT starting point is less accurate: after the first iteration, the frequency error is 9·6% while the loss factor is 97·9% too low. However, even with the FSDT starting point, after three iterations the error is effectively eliminated.

Figure 4 shows the transverse shear stress distribution for length to thickness ratios of $S = 10$ and $S = 2$. In the figure, z is non-dimensionalized by the beam half thickness and the shear stress is normalized by the maximum stress. For $S = 10$, the location of the damping layer can be identified as the region of constant shear stress. The shear stress is

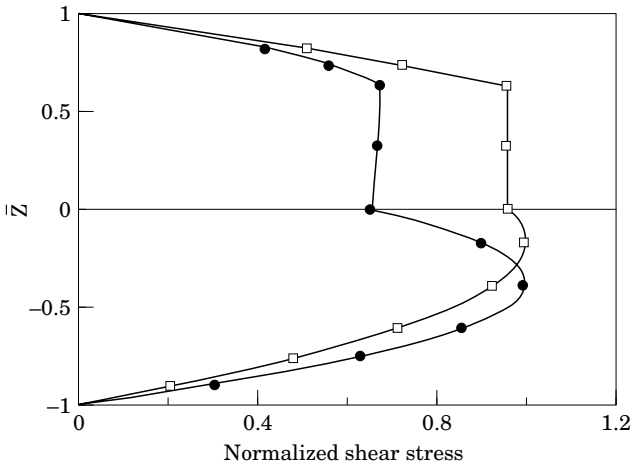

Figure 4. Transverse shear stress distribution for three layer example: □, length to thickness ratio, $S = 10$; ●, $S = 2$.

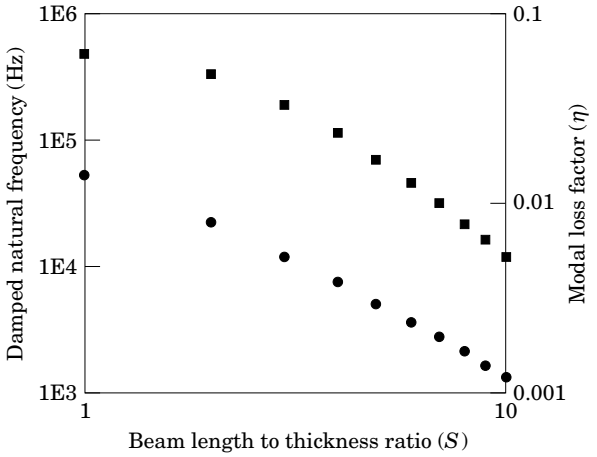

Figure 5. Modal data for nine layer example: ●, ISLM frequency; ■, ISLM loss factor.

constant in the damping layer because the shear gradient, from equation (14), is effectively zero. The in-plane gradient is zero because $E_{\text{core}} = 0$ and the inertial term is small because the modal frequency is low. For $S = 2$, because of the higher modal frequency, the inertial term in equation (14) is large enough to produce a small shear gradient in the core which is evident in the figure.

3.2. NINE LAYER EXAMPLE

The ISLM is readily adaptable to multiple layer configurations; all that is required is the specification of the material property distribution through the thickness. In order to demonstrate a multi-ply example, Rao's beam was modified such that the shear core was split into four equal thickness (1·25 mm) layers. The core layers were interspersed among five equal thickness (2·2 mm) layers of the facesheet material. The total thickness of core and facesheet material was 5.0 mm and 11·0 mm, respectively, the same as the original beam.

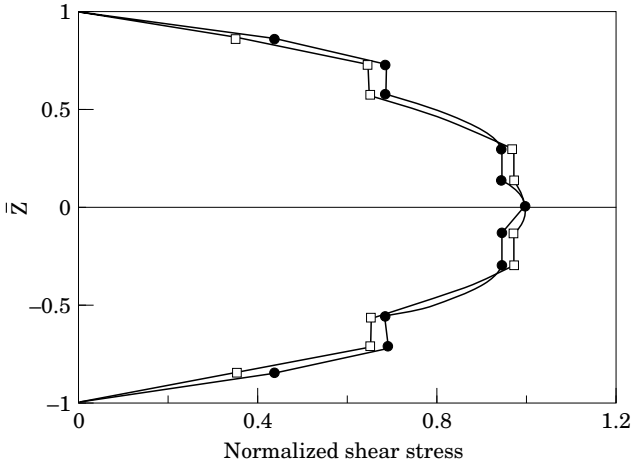

Figure 6. Transverse shear stress distribution for nine layer example: □, length to thickness ratio, $S = 10$; ●, $S = 2$.

The modal data for the nine layer beam appears in Figure 5. For $S = 10$, the modal frequency for the nine layer beam is approximately 10% lower than the three layer beam, however, the loss factor is double. For shorter wavelengths, there is very little frequency difference, however, the nine layer loss factors are approximately 20% lower than the three layer beam. The improved damping performance at low frequency occurs because the beam is "softened" in shear, placing more strain energy in the dissipative core material. At high frequency, the damping material is more effectively located near the beam's neutral axis where the shear stress is maximum.

Figure 6 shows the shear stress distributions for the nine layer beam with length-to-thickness ratios of $S = 10$ and $S = 2$. Unlike the 3 layer beam, the shear stress distributions were similar for both beam lengths. The location of the four damping layers can be seen in the figure as regions of constant shear stress.

4. CONCLUSIONS

A smeared laminate beam model has been presented that can accurately determine the dynamic stress distribution in general laminated beams. This represents an advance over previous smeared laminate models, in which accurate estimates of the stress field were only possible if the assumed displacement field was a reasonable approximation of the actual displacement field.

REFERENCES

1. P. C. Yang, C. H. Norris and Y. Stavsky 1966 *International Journal of Solids and Structures* **2**, 665–684. Elastic wave propagation in heterogeneous plates.
2. A. V. Krishna Murty 1970 *American Institute of Aeronautics and Astronautics Journal* **8**, 34–38. Vibrations of short beams.
3. M. Levinson 1981 *Journal of Sound and Vibration* **74**, 81–87. A new rectangular beam theory.
4. M. Levinson 1981 *Journal of Sound and Vibration* **77**, 440–444. Further results of a new beam theory.
5. J. N. Reddy 1984 *Journal of Applied Mechanics* **51**, 745–752. A simple higher-order theory for laminated composite plates.
6. M. Di Sciuva 1986 *Journal of Sound and Vibration* **105**, 425–442. Bending, vibration and buckling of simply supported thick multilayered orthotropic plates: an evaluation of a new displacement model.
7. K. Bhaskar and T. K. Varadan 1989 *American Institute of Aeronautics and Astronautics Journal* **27**, 1830–1831. Refinement of higher-order laminated plate theories.
8. D. Ross, E. E. Ungar and E. M. Kerwin 1959 *Structural Damping*, 48–87. New York: ASME. Flexural vibrations by means of viscoelastic laminae.
9. C. Sun and J. M. Whitney 1973 *American Institute of Aeronautics and Astronautics Journal* **11**, 178–183. Theories for the dynamic response of laminated plates.
10. N. Alam and N. T. Asnani 1987 *Journal of Sound and Vibration* **119**, 347–362. Refined vibration and damping analysis of multilayered rectangular plates.
11. J. N. Reddy 1987 *Communications in Applied Numerical Methods* **3**, 173–180. A generalization of two-dimensional theories of laminated composite plates.
12. A. K. Noor and W. S. Burton 1989 *Composite Structures* **11**, 183–204. Stress and free vibration analyses of multilayered composite plates.
13. K. Vijayakumar and A. V. Krishna Murty 1988 *Composite Science and Technology* **32**, 165–181. Iterative modeling for stress analysis of composite laminates.
14. J. A. Zapfe and G. A. Lesieutre 1996 *American Institute of Aeronautics and Astronautics Journal*. **34,** 1299–1301. Iterative calculation of the transverse shear distribution in laminated composite beams.
15. D. K. Rao 1978 *Journal of Mechanical Engineering Science* **20**, 271–282. Frequency and loss factors of sandwich beams under various boundary conditions.
16. D. J. Mead and S. Markus 1969 *Journal of Sound and Vibration* **10**, 163–175. The forced vibration of a three-layer, damped sandwich beam with arbitrary boundary conditions.